Electronic Supplementary Material (ESI) for Journal of Materials Chemistry A.
This journal is © The Royal Society of Chemistry 2023

Supporting information

Nanoarchitectonics Tuning for Fe/N Doped C_{60}-Derived Carbon Electrocatalysts with Enhanced ORR Activity by Oxygen Plasma Treatment on C_{60}

Li Ju,[a#] Gazi Hao,[b#] Fancang Meng,[a] Wei Jiang,[b*] Qingmin Ji [a*]

[a] *Herbert Gleiter Institute for Nanoscience, School of Materials Science and Engineering, Nanjing University of Science & Technology, 200 Xiaolingwei, Nanjing, 210094, China*

[b] *National Special Superfine Powder Engineering Technology Research Center, Nanjing University of Science and Technology, 200 Xiaolingwei, Nanjing, 210094, China*

[#] These authors contributed this work equally

Corresponding author: *superfine_jw@126.com; jiqingmin@njust.edu.cn*

Supplementary Data

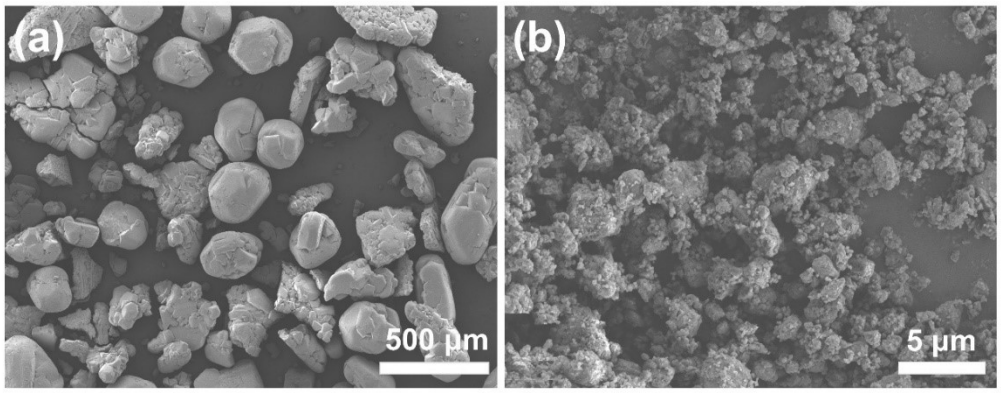

Fig. S1. The SEM images of (a) pristine C_{60} before grinding, (b) pristine C_{60} after grinding.

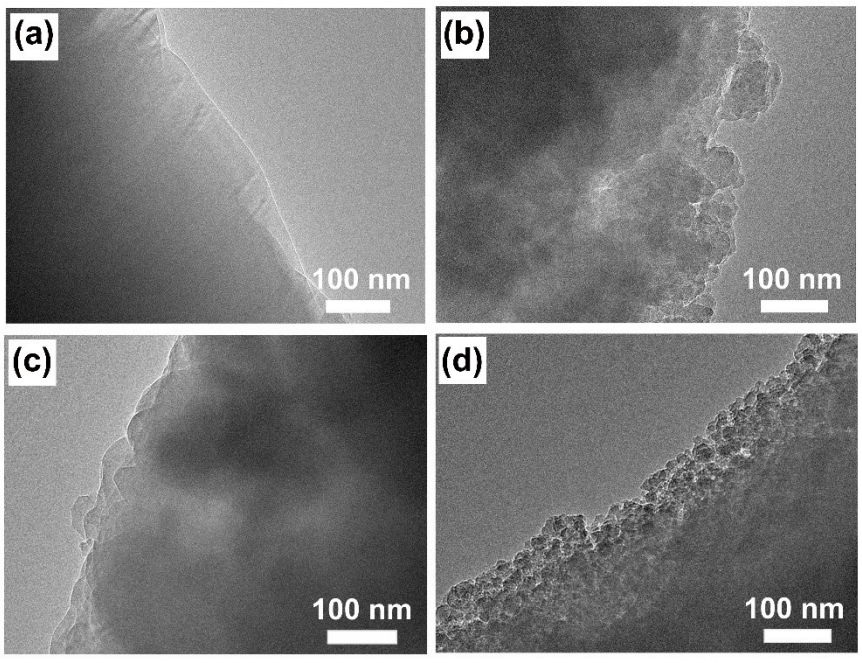

Fig. S2. The TEM images of (a) C_{60}, (b) $C_{60}O$, (c) Fe-C_{60}, and (d) Fe-$C_{60}O$.

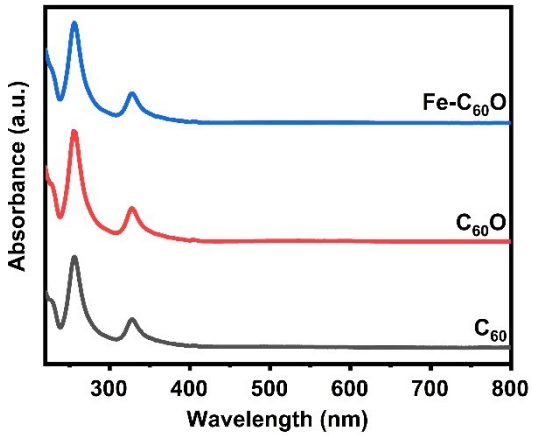

Fig. S3. The UV-Vis Spectra of C_{60}, $C_{60}O$ and Fe-$C_{60}O$ from 220 to 800 nm in *n*-hexane.

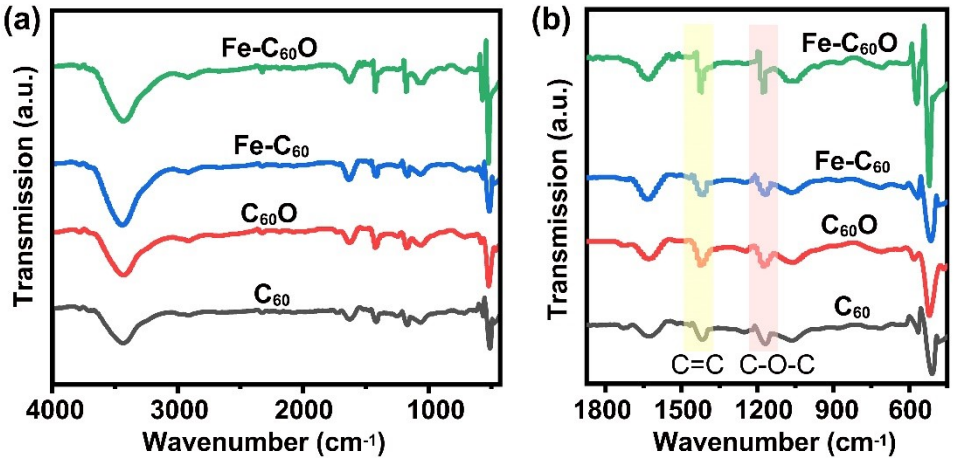

Fig. S4. (a) The FTIR spectra of C_{60}, $C_{60}O$, Fe-C_{60} and Fe-$C_{60}O$ in the range of 400–4000 cm^{-1}. (b) The enlarge spectra in the range of 450–2000 cm^{-1}.

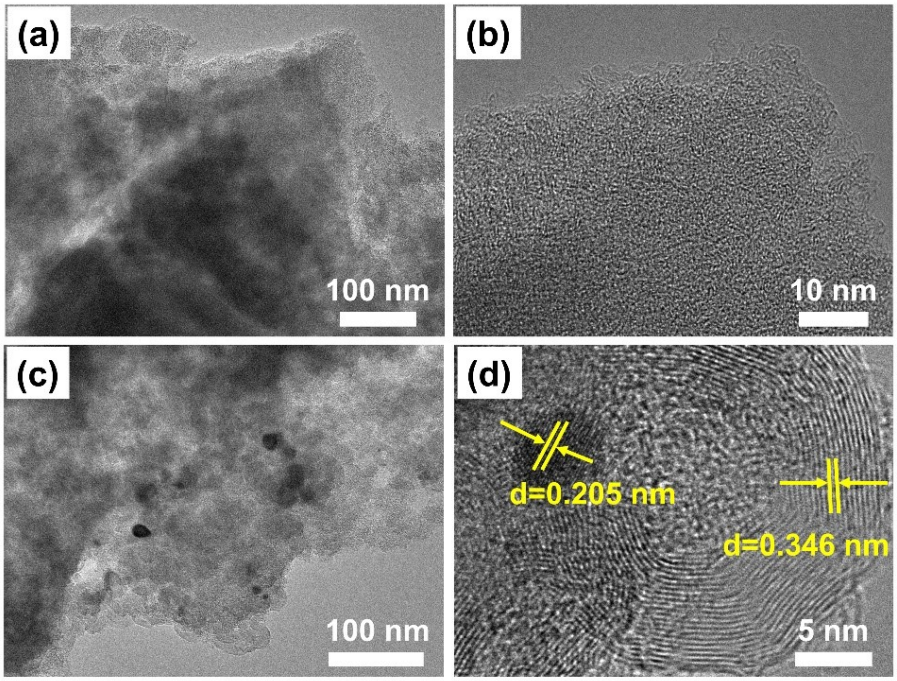

Fig. S5. The TEM images of (a) Fe/C_{60}-900 and (c) Fe/C_{60}O-900. The HR-TEM images of (b) Fe/C_{60}-900 and (d) Fe/C_{60}O-900.

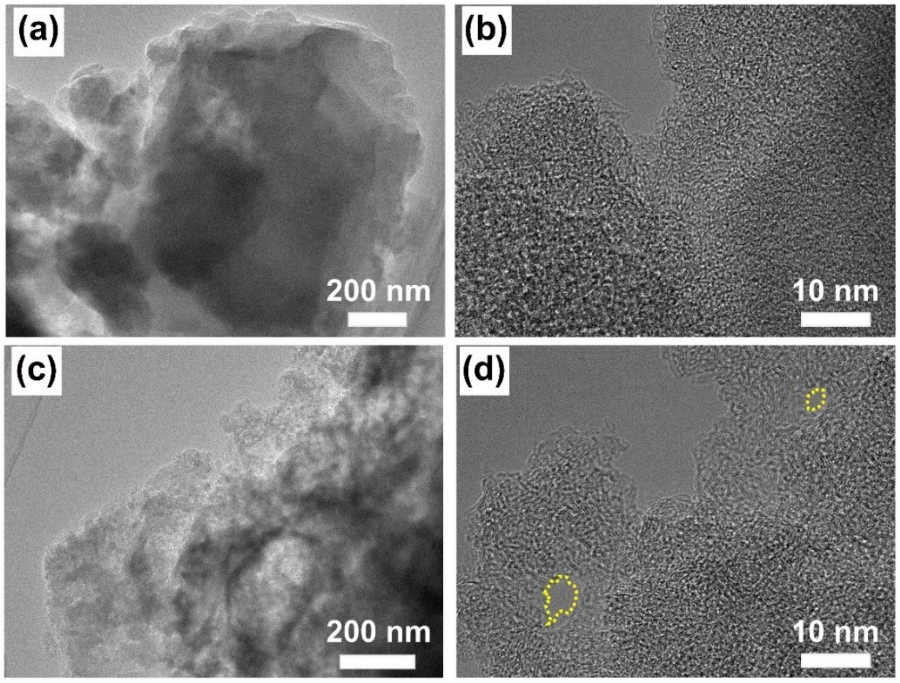

Fig. S6. The TEM images of (a) $C_{60}O$-900 and (c) N/$C_{60}O$-900. The HR-TEM images of (b) $C_{60}O$-900 and (d) N/$C_{60}O$-900.

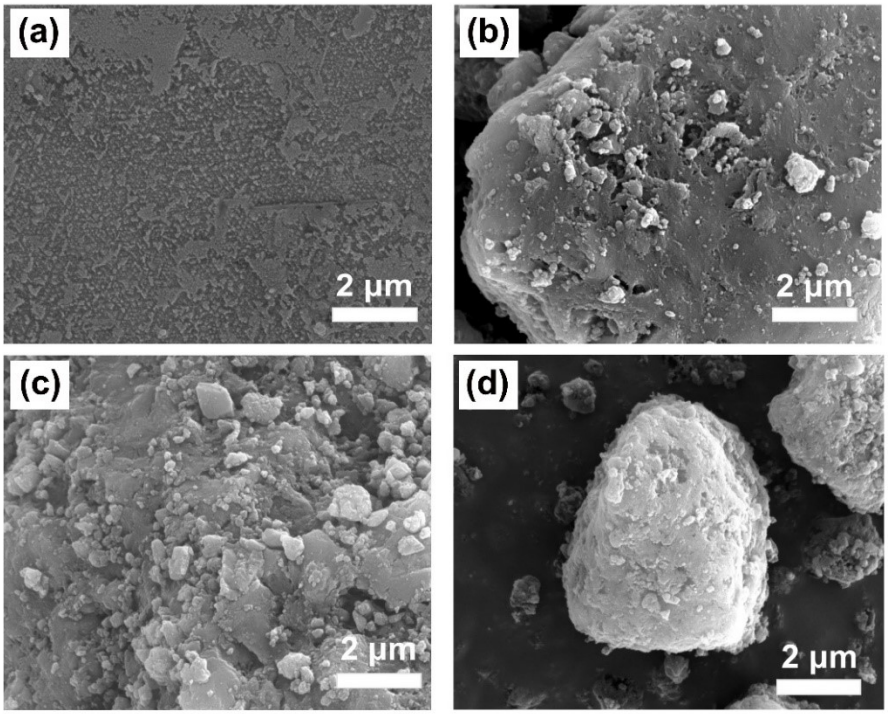

Fig. S7. The SEM images of (a) Fe/C_{60}-900, (b) C_{60}O-900, (c) Fe/C_{60}O-900, and (d) N/C_{60}O-900.

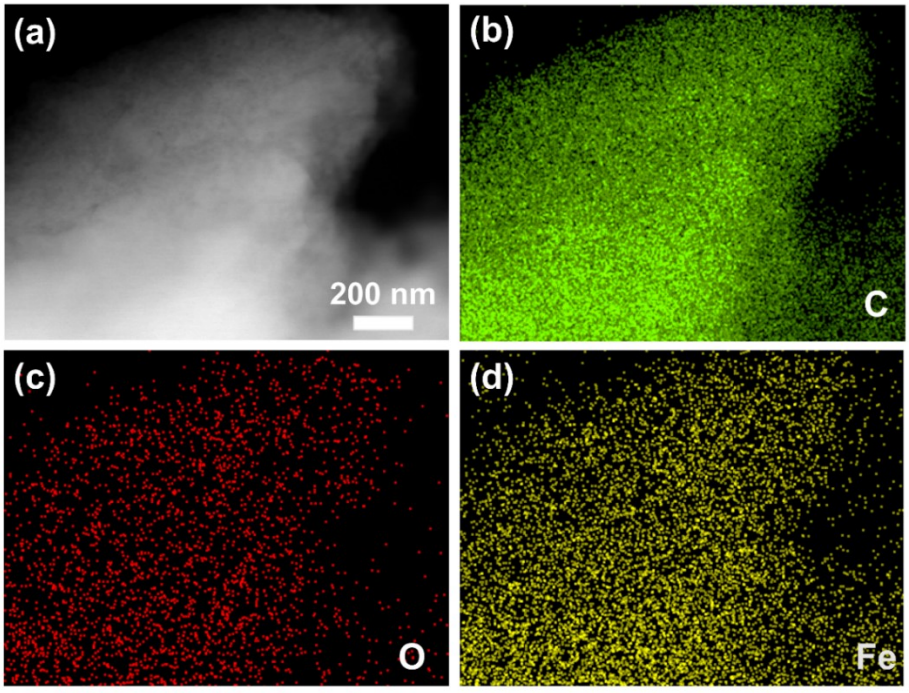

Fig. S8. (a) The HAADF-STEM image of Fe-C_{60}O and the corresponding elemental mappings of (b) C, (c) O and (d) Fe.

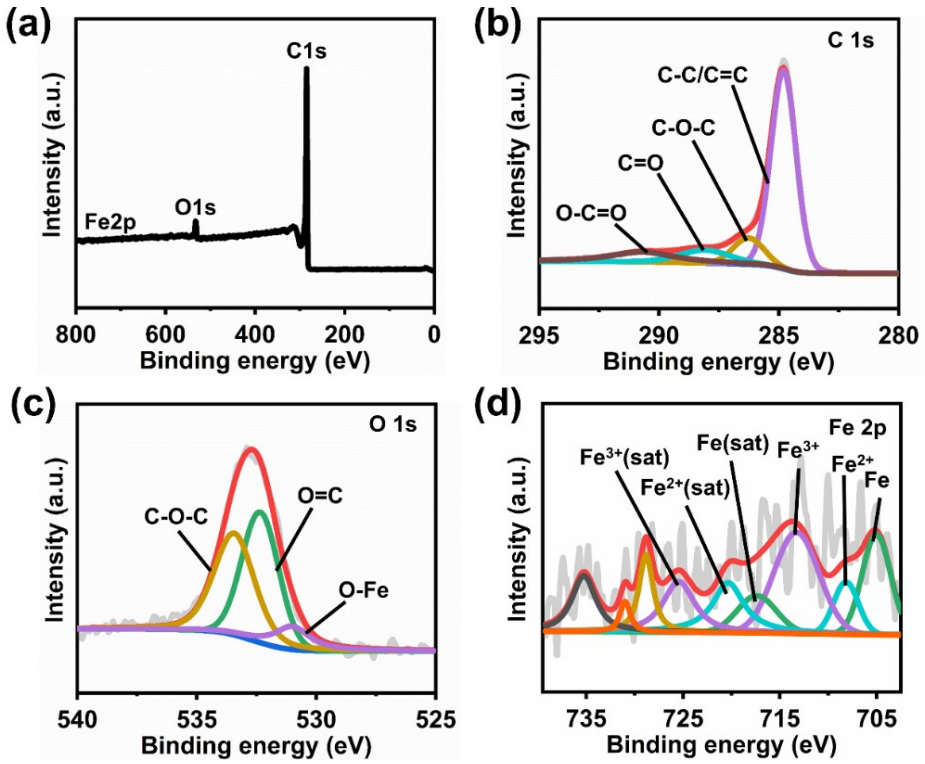

Fig. S9. (a) The XPS survey spectrum of Fe/C_{60}O-900. The (b) C 1s, (c) O 1s, (d) Fe 2p XPS spectra of Fe/C_{60}O-900.

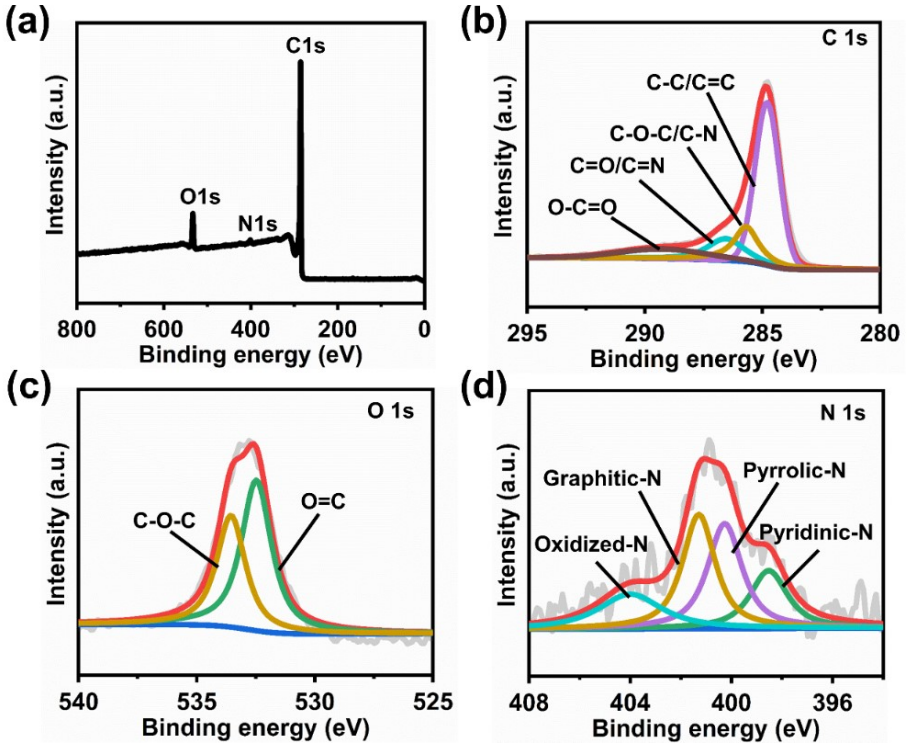

Fig. S10. (a) The XPS survey spectrum of N/C_{60}O-900. The (b) C 1s, (c) O 1s, (d) N 1s XPS spectra of N/C_{60}O-900.

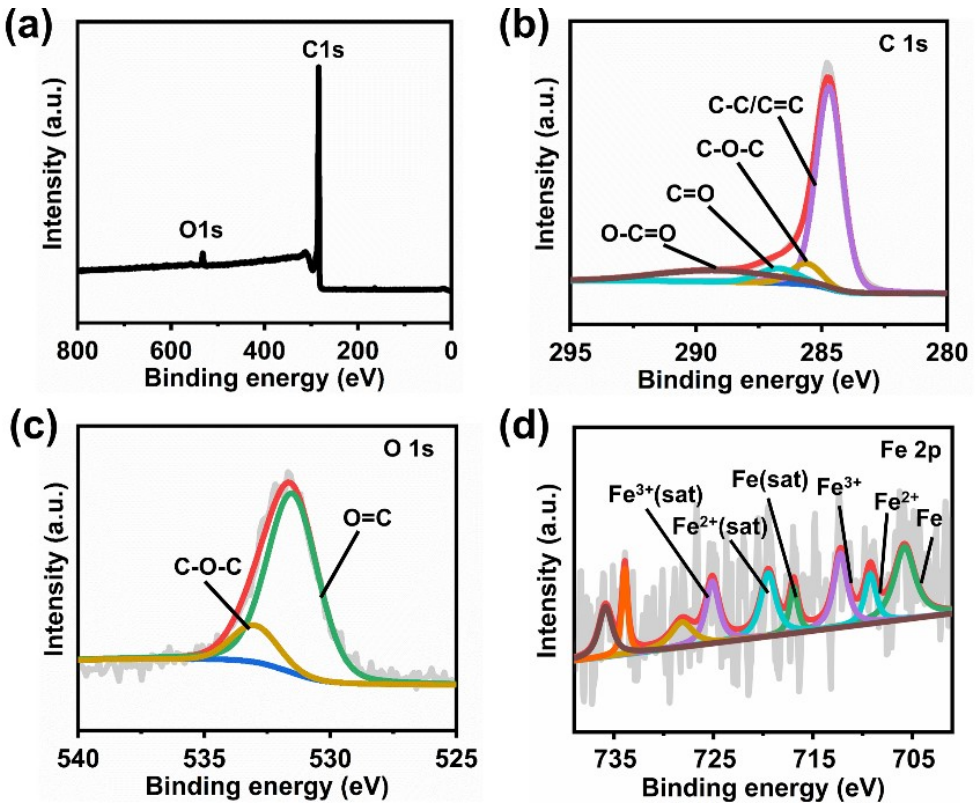

Fig. S11. (a) The XPS survey spectrum of Fe/C_{60}-900. The (b) C 1s, (c) O 1s, (d) Fe 2p XPS spectra of Fe/C_{60}-900.

Table S1. The calculated proportion of various Fe states in Fe containing C_{60}-derived carbons based on the Fe 2p XPS spectra.

Sample name	Fe	Fe^{2+}	Fe^{3+}	Fe-N
Fe/C_{60}-900	36.1%	29.2%	34.7%	-
Fe/C_{60}O-900	29.3%	24.7%	46.0%	-
FeN/C_{60}O-900	25.6%	26.4%	29.0%	19.0%

Table S2. The comparison of N, Fe contents in different reported C_{60}-derived carbon electrocatalysts

Sample name	XPS, N %	XPS, Fe %	ICP, Fe %	*Ref.*
FeN/C_{60}O-900	2.62	0.16	4.94	This work
FeN@FCS-900	1.91	0.43	6.07	[1]
FMN700	1.6	3.6	-	[2]
MN7-10/3	1.64	0.62	-	[3]
Fe-MFC_{60} -150	-	1.4	-	[4]
NP^3@CHS	3.44	-	-	[5]
N,S-PCNFs	4.03	-	-	[6]
N,S-PHCNSs-75	2.88	-	-	[7]
C_{60}@Co-N-PCM	2.1	-	-	[8]

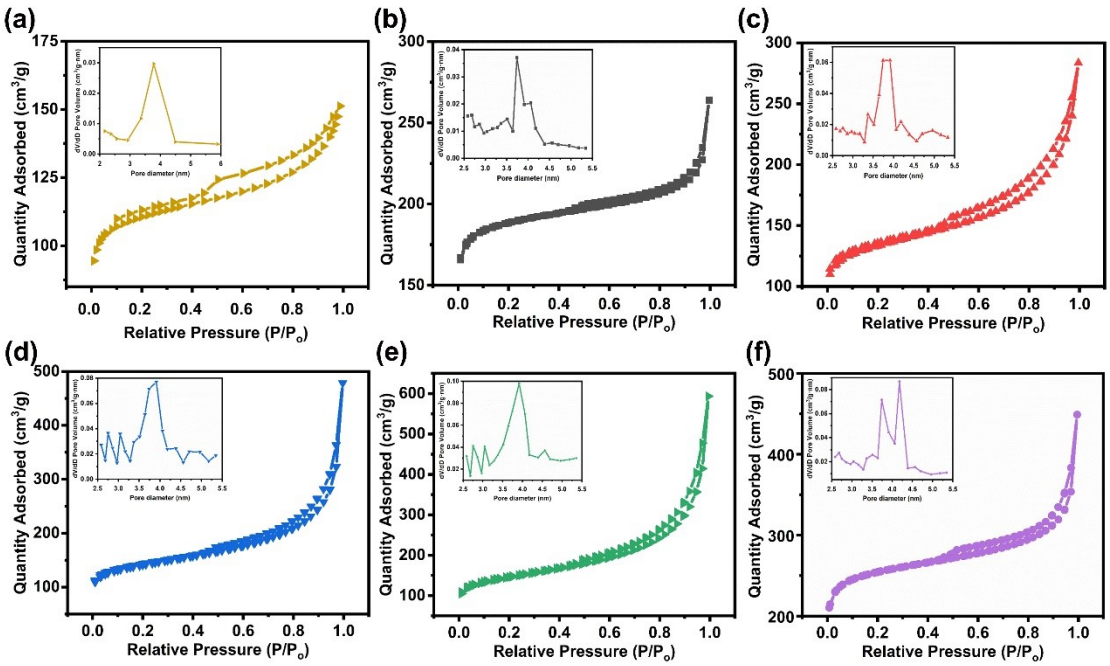

Fig. S12. The N_2 sorption isotherms and pore size distribution curves (inset) of (a) C_{60}-900, (b) $C_{60}O$-900, (c) Fe/C_{60}-900, (d) Fe/$C_{60}O$-900, (e) N/$C_{60}O$-900 and (f) FeN/$C_{60}O$-900.

Table S3. The porous characteristic properties of C_{60}-900, $C_{60}O$-900, Fe/C_{60}-900, Fe/$C_{60}O$-900, N/$C_{60}O$-900 and FeN/$C_{60}O$-900 based on nitrogen sorption measurements

Sample name	**BET surface area** ($m^2\ g^{-1}$)	**Average pore size** (nm)	**Pore volume** ($cm^3\ g^{-1}$)
C_{60}-900	435	6.17	0.080
$C_{60}O$-900	596	4.06	0.121
Fe/C_{60}-900	431	5.88	0.260
Fe/$C_{60}O$-900	463	6.56	0.453
N/$C_{60}O$-900	484	9.56	0.844
FeN/$C_{60}O$-900	810	4.87	0.297

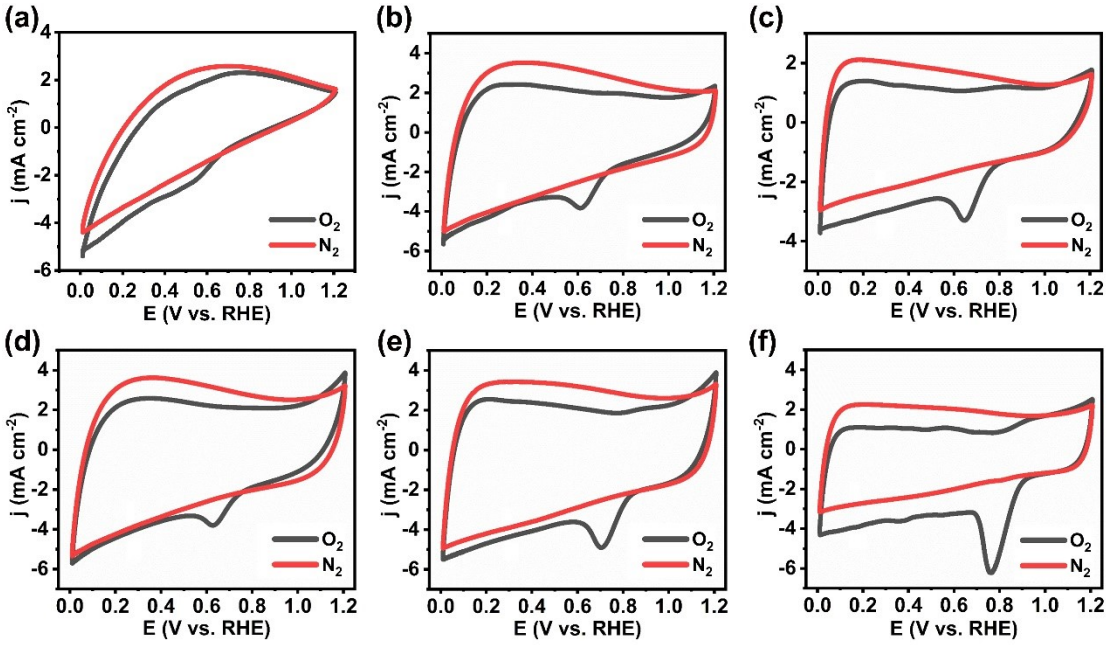

Fig. S13. The CV curves of (a) C_{60}-900, (b) Fe/C_{60}-900, (c) C_{60}O-900, (d) Fe/C_{60}O-900, (e) N/C_{60}O-900 and (f) FeN/C_{60}O-900 in N_2 and O_2-saturated 0.1 mol·L^{-1} KOH.

Table S4. The comparison of ORR activities of C_{60}-900, C_{60}O-900, Fe/C_{60}-900, Fe/C_{60}O-900, N/C_{60}O-900, FeN/C_{60}O-900 and Pt/C

Sample name	E_0 (V)	$E_{1/2}$ (V)	j_L (mA·cm^{-2})
C_{60}-900	0.75	0.56	2.05
Fe/C_{60}-900	0.80	0.64	3.27
C_{60}O-900	0.81	0.68	3.39
Fe/C_{60}O-900	0.83	0.70	3.69
N/C_{60}O-900	0.89	0.78	4.23
FeN/C_{60}O-900	0.98	0.85	5.23
Pt/C	0.98	0.83	5.13

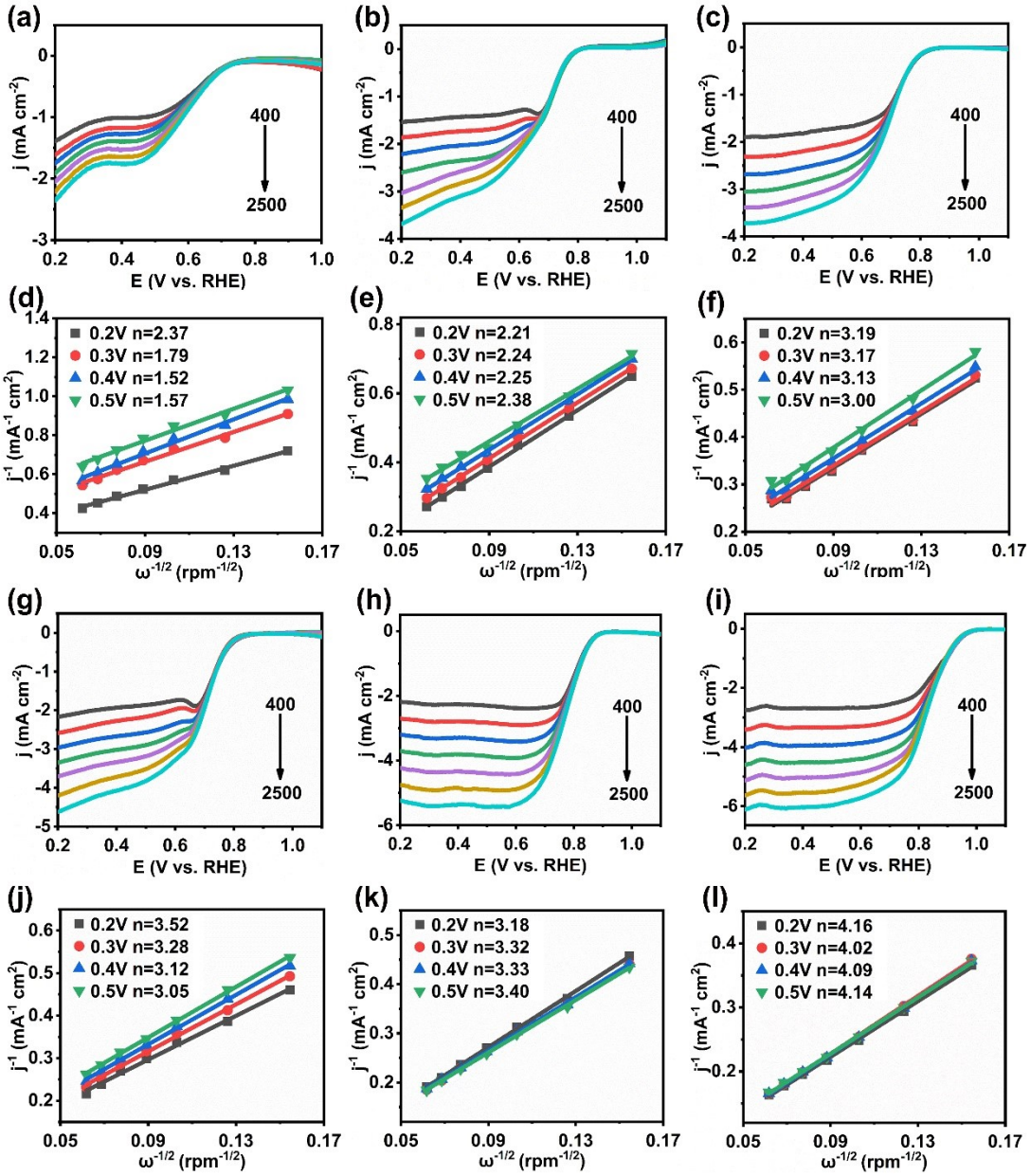

Fig. S14. The LSV curves of (a) C_{60}-900, (b) Fe/C_{60}-900, (c) C_{60}O-900, (g) Fe/C_{60}O-900, (h) N/C_{60}O-900 and (i) Pt/C at a series of rotation speeds from 400 rpm to 2500 rpm. The K-L plots of (d) C_{60}-900, (e) Fe/C_{60}-900 (f) C_{60}O-900, (j) Fe/C_{60}O-900 a), (k) N/C_{60}O-900 and (l) Pt/C.

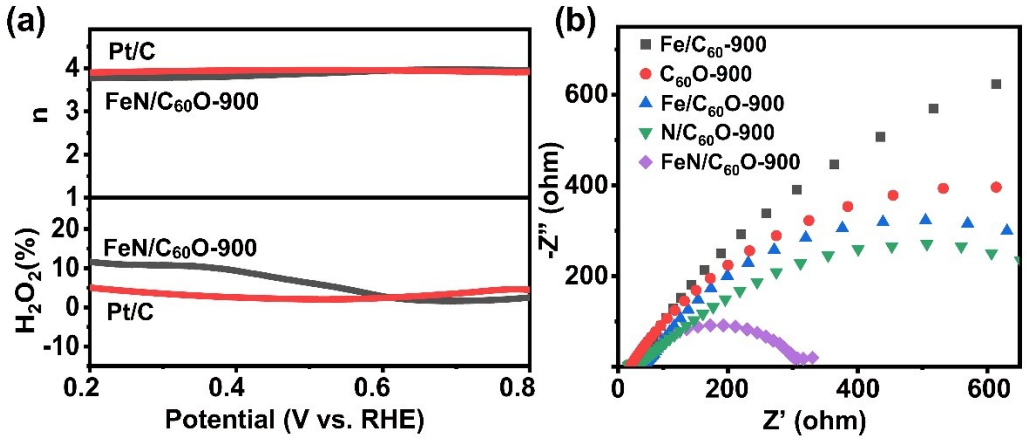

Fig. S15. (a) The electron transfer number (n) and H_2O_2% yield of FeN/C_{60}O-900 and Pt/C. (b) The Nyquist plots of FeN/C_{60}O-900, N/C_{60}O-900, Fe/C_{60}O-900, C_{60}O-900, and Fe/C_{60}-900.

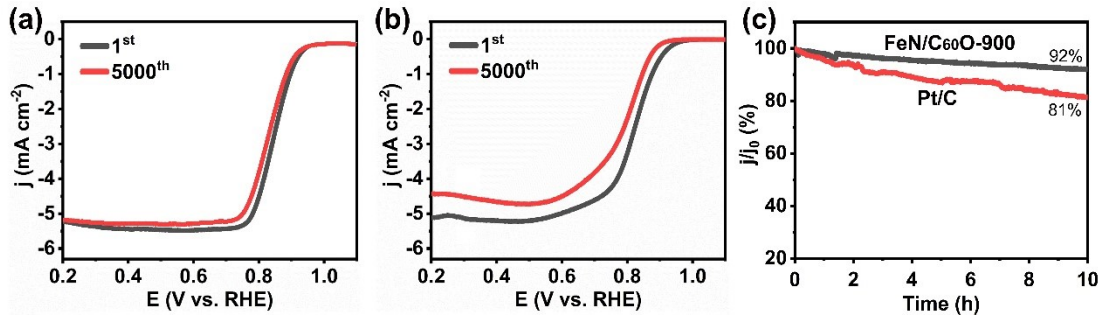

Fig. S16. The LSV curves of (a) FeN/C_{60}O-900 and (b) Pt/C in O_2-saturated 0.1 M KOH solution at 1600 rpm; before and after 5000 potential cycles. (c) The *i*–t response curves of FeN/C_{60}O-900 and Pt/C.

Table S5. The comparison of the ORR performance of the reported metal-doped C_{60}-derived carbons in alkaline medium.

Sample name	E_0 (V)	$E_{1/2}$ (V)	j_L (mA·cm^{-2})	***Ref.***
FeN/C_{60}O-900	0.98	0.85	5.23	This work
FeN@FCS-900	0.93	0.78	4.2	[1]
FMN700	0.93	0.81	4.7	[2]
Fe-MFC_{60} -150	0.85	0.78	3	[4]
C_{60}@Co-N-PCM	0.98	0.85	5.5	[8]
C_{60}/FeTPP-700	0.98	0.88	5.4	[9]

References (in supporting information)

[1] B. Jiang, S. Wang, F. Meng, L. Ju, W. Jiang, Q. Ji and H. D. Quan, *CrystEngComm*, 2022, **24**, 5783-5791.

[2] Z. Peng, Q. Jiang, P. Peng and F.-F. Li, *Eng. Sci.*, 2021, **14**, 27-38.

[3] A. Yu, Z. Peng, Y. Li, L. Zhu, P. Peng and F.-F. Li, *ACS Appl. Mater. Interfaces*, 2022, **14**, 42337−42346

[4] M. R. Benzigar, S. Joseph, G. Saianand, A.-I. Gopalan, S. Sarkar, S. Srinivasan, D.-H. Park, S. Kim, S. N. Talapaneni and K. Ramadass, *Microporous Mesoporous Mater.*, 2019, **285**, 21-31.

[5] F. Meng, S. Wang, B. Jiang, L. Ju, H. Xie, W. Jiang and Q. Ji, *Nanoscale*, 2022, **14**, 10389-10398.

[6] Z. He, P. Wei, N. Chen, J. Han and X. Lu, *Chem.-Eur. J.*, 2021, **27**, 1423-1429.

[7] Z. He, P. Wei, T. Xu, J. Han, X. Gao and X. Lu, *Mater. Chem. Front.*, 2021, **5**, 7873-7882.

[8] J. Wu, S. Wang, Z. Lei, R. Guan, M. Chen, P. Du, Y. Lu, R. Cao and S. Yang, *Nano Res.*, 2021, **14**, 2596-2605.

[9] H. Wang, L. Cao, Y. Feng, J. Chen,W. Feng, T. Luo, Y. Hu, C. Yuan, Y. Zhao, Y. Zhao, K. Kajiyoshi, Y. Liu, Z. Li and J. Huang, *Chin. Chem. Lett.*, 2023, **34**, 107601.